Journal of
Micro/Nanolithography,
MEMS, and MOEMS

SPIEDigitalLibrary.org/jm3

Metrological scanning probe microscope based on a quartz tuning fork detector

Bakir Babic
Christopher H. Freund
Jan Herrmann
Malcolm A. Lawn
John Miles

SPIE

Metrological scanning probe microscope based on a quartz tuning fork detector

Bakir Babic
Christopher H. Freund
Jan Herrmann
Malcolm A. Lawn
John Miles
National Measurement Institute Australia
P.O. Box 264
Lindfield, NSW 2070, Australia
E-mail: malcolm.lawn@measurement.gov.au

Abstract. We give an overview of the design of a metrological scanning probe microscope (mSPM) currently under development at the National Measurement Institute Australia (NMIA) and report on preliminary results on the implementation of key components. The mSPM is being developed as part of the nanometrology program at NMIA and will provide the link in the traceability chain between dimensional measurements made at the nanometer scale and the realization of the International System of Units (SI) meter at NMIA. The instrument is based on a quartz tuning fork (QTF) detector and will provide a measurement volume of 100 μm $\times$ 100 μm $\times$ 25 μm with a target uncertainty of 1 nm for the position measurement. Characterization results of the nanopositioning stage and the QTF detector are presented along with an outline of the method for tip mounting on the QTFs. Initial imaging results are also presented. © *2012 Society of Photo-Optical Instrumentation Engineers (SPIE).* [DOI: 10.1117/1.JMM.11.1.011003]

Subject terms: metrological scanning probe microscope; atomic force microscopy; noncontact mode; quartz tuning fork; frequency modulation.

Paper 11074SSP received May 20, 2011; revised manuscript received Sep. 20, 2011; accepted for publication Sep. 23, 2011; published online Mar. 2, 2012.

1 Introduction

The National Measurement Institute Australia (NMIA) is establishing a capability in measurement at the nanometer scale with the aims of supporting research, development, and commercial application of nanotechnology in Australia and to assist in ensuring the safety of applications of nanotechnology for Australian consumers, workplaces, and the environment. To achieve these aims, NMIA is creating two new facilities—a scanning probe microscopy (SPM) metrology laboratory and a nanoparticle characterization laboratory.

The purpose of the SPM metrology laboratory is to link dimensional measurements made at the nanometer scale with the realization of the International System of Units (SI) meter at NMIA. The keyelement of this link is a metrological scanning probe microscope (mSPM), which combines the precision of dimensional measurements achievable with SPM with the accuracy achievable by laser interferometry. Traceable dimensional metrology at the macroscopic scale is technologically mature; however, the emergence of nanotechnology requires such measurements at the nanometer scale. Conventional SPMs can readily achieve nanometer scale precision, and by incorporating laser interferometry into an mSPM, traceability to the realization of the SI meter can be achieved.[1,2]

The challenge in realizing this mSPM concept is to create a macroscopic mechanical instrument capable of traceable dimensional measurement at the nanoscale with a combined uncertainty of less than 1 nm. Experience in designing ultraprecision mechanical stages and instruments[3] and in operating similar mSPMs at other metrology institutes[4–9] has shown that there are many contributions to the uncertainty of the displacement measurements. These include alignment errors (particularly Abbé errors[10]), deformations of the mechanical structures (for instance, due to thermal expansion), motion errors of the translation stage, form errors of the interferometer mirrors, nonlinearities of the interferometers, and fluctuations in the refractive index of air.

In this paper, we present an overview of the design and operation of the mSPM, highlight the issues specifically associated with an instrument based on a quartz tuning fork (QTF) detector, and present characterization results of some of the components and preliminary imaging.

2 Instrument Components and Design Principle

The mSPM comprises the following components: (1) a metrological frame that defines the reference coordinate system, (2) translation stages to implement the displacement between the probe and the sample, (3) differential plane mirror interferometers to measure the displacement, (4) a detector with a sharp tip and a sensor to quantify the interaction between tip and sample, and (5) a feedback system to maintain the interaction at a fixed level and to control the relative position between probe and sample (that is, the scanning motion). Figure 1 shows some of the main mSPM components.

The instrument design follows a number of principles that are aimed at minimizing the magnitude of the contributions to the total uncertainty. For example, to minimize the Abbé offsets and associated errors, the probe tip is fixed with respect to the metrological frame, and the interferometers are aligned such that their beams virtually intersect at the tip.

2.1 *Translation Stage*

Translation stages are commercially available for research-grade SPMs, optical microscopy, lithography, optical fiber alignment, and other applications requiring subnanometer

0091-3286/2012/$25.00 © 2012 SPIE

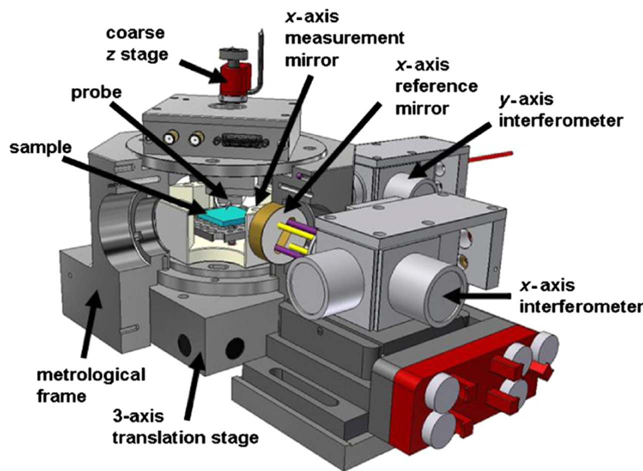

Fig. 1 Main components of the mSPM. The *Z*-axis interferometer, which is located below the translation stage, is not shown in this cutaway illustration.

resolution positioning. A translation stage has been selected for the NMIA mSPM* with an *XY*-axes scan range of 100×100 μm and a range in the *Z*-axis of 25 μm.[11] The stage features an aperture in the *Z*-axis for optical access.

The translation stage consists of a central moving platform linked to a static base with flexure hinges that guide the motion by deformation of the flexure material, thereby allowing smooth friction and stiction-free motion. Flexure hinges are arranged to minimize out-of-plane motion, tilting errors, and crosstalk. Nevertheless, these imperfections in stage motion can never be completely eliminated, and to achieve the required accuracy of the mSPM, it will be necessary to survey the full range of motion of the translation stage with laser interferometry to establish a set of corrections.

Piezoelectric actuators between the static base and the moving platform provide the motion that is controlled by voltage signals applied to each of the actuators. A dedicated controller provides a preprogrammed signal for *XY*-axis scanning and, from the feedback signal originating from the probe tip, applies the appropriate voltage to the *Z*-axis actuator to follow the sample surface topography. Ideally, piezoelectric actuators expand proportionally to the voltage applied. However, in reality, they exhibit nonlinearity, hysteresis, and creep, resulting in errors in positioning that are significant at the resolution required. The translation stage has the capability of closed-loop operation, whereby the position of the moving platform is monitored by either capacitive sensors incorporated into the stage or external sensors such as interferometers. This allows the controller to correct for these positioning errors by adjusting the voltages applied to the actuators. The mSPM design also incorporates angle interferometers opposite the *X*-axis and *Y*-axis linear displacement interferometers to measure the angular stage errors.

The requirement to implement closed-loop control of the tip-sample interaction based on the motion of the translation stage places significant design constraints on the mSPM. To keep the mechanical resonance frequencies of the combined translation stage—mirror—sample assembly as high as possible, thereby reducing the coupling of the scanning motion to the vibration modes of the stage, the mass load on the translation stage has to be kept to a minimum. The design of both the sample holder and the mirror assembly minimizes their respective masses, which combined will be 214 g, while maintaining their mechanical integrity and stiffness. The mechanical resonance frequencies of the translation stage for motion along the *X*-, *Y*-, and *Z*-axes have been measured both unloaded and with a 214-g load, simulating the combined mass of the mirror assembly and the sample stage. The frequency responses of the nanopositioning stage for motion along the three axes are shown in Fig. 2, and the values of the resonance frequencies are given in Table 1. It is anticipated that the maximum mass of a transfer standard artifact examined with the mSPM will be less than 10 g.

For the *X*- and *Y*-axes, the loading of the mirror assembly and the sample stage reduces the resonance frequency of the nanopositioning stage by approximately 25%, while for the *Z*-axis, the resonance frequency is reduced by 40%. Without knowing the internal design of the nanopositioning stage, which is proprietary information, it is difficult to determine the origin of this difference; however, it is consistent with the flexure hinges of the stage's translation mechanism in the *Z*-axis being stiffer, due to design constraints on their size, than the flexure hinges in the *X*- and *Y*-axes. The loaded resonance frequency in the *Z*-axis of 961 Hz allows operation of the mSPM at moderate scan rates. Our experience has shown that it is possible to reliably scan at a rate of 1 Hz and a resolution of 512 points per scan line.

2.2 *QTF Detector*

The mSPM operates in a dynamic noncontact atomic force microscopy (AFM) mode and uses a tip mounted on an oscillating QTF as a probe.[12] Operating in noncontact mode greatly reduces the problem of tip wear and sample surface degradation associated with the classic contact mode

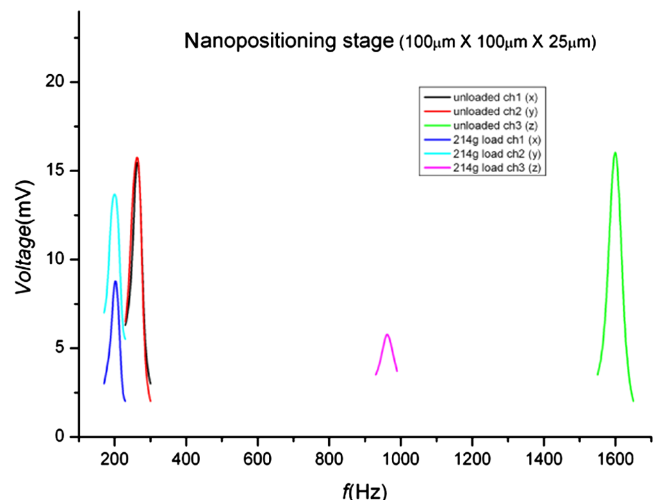

Fig. 2 The frequency responses of the nanopositioning stage for each of the axes (*X*, *Y*, and *Z*) both unloaded and with a 214-g load simulating the combined mass of the mirror assembly and the sample stage. Each axis has been driven with 20-mV peak-to-peak sinusoidal excitation.

*Certain commercial products are identified in this publication. Such identification does not imply recommendation or endorsement by the National Measurement Institute Australia, nor does it imply that the materials or equipment identified are necessarily the best available for the purpose.

Table 1 Measured resonance frequencies in the three displacement axes of the nanopositioning stage both unloaded and with a load of 214 g simulating the combined mass of the mirror assembly and the sample stage. Each axis has been driven with a 20-mV peak-to-peak sinusoidal excitation.

Axes	Resonance frequency (Hz)	
	Unloaded	Load 214 g
X	263.1	202.1
Y	265.5	200.6
Z	1599.3	961.4

configuration. In a scanning probe microscope, a QTF can serve both as actuator and sensor of tip-sample interaction. The motion of the QTF can be generated either piezoelectrically by an AC voltage drive or mechanically by oscillating the QTF with an external actuator at or near the QTF resonance frequency. The QTF oscillations are sensed by monitoring the current through the QTF.

A QTF probe has been chosen to reduce both heat dissipation in the instrument and complexity of the AFM probe head since, unlike for systems with mechanical excitation and conventional "beam bounce" detector configurations, it requires neither a "shaker" piezo actuator nor a laser and position-sensitive detector to read-out cantilever deflection. SPMs operating in this configuration have achieved subatomic resolution.[13] An optical micrograph of a QTF used in the mSPM is shown in Fig. 3(a). As shown in Fig. 3(b), a tip is mounted perpendicular to one of the QTF tines. Our instrument operates the QTF probe in a frequency modulation (FM) mode where the probe vibrates at its resonance frequency. As the tip comes into close proximity to the sample surface, the attractive van der Waals force between the tip and the sample surface causes a measurable shift in the frequency, amplitude, and phase of the oscillation.[14–16]

2.3 *Tip-mounting Procedure and Characterization*

We have developed a systematic and reproducible method to attach AFM cantilevers with tips to the QTFs for use in the mSPM. The performance of the tuning forks with attached

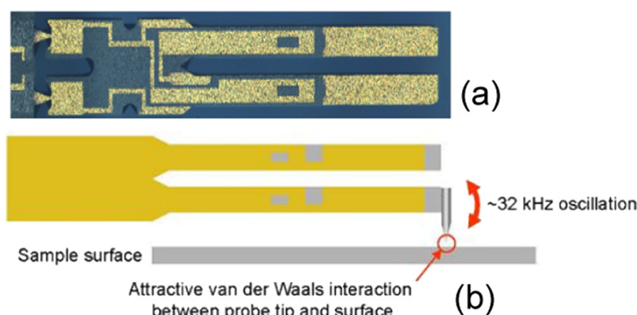

Fig. 3 (a) Optical micrograph of a QTF oscillator (with a 3.67-mm total length). (b) Schematic diagram of the dynamic noncontact AFM mode.

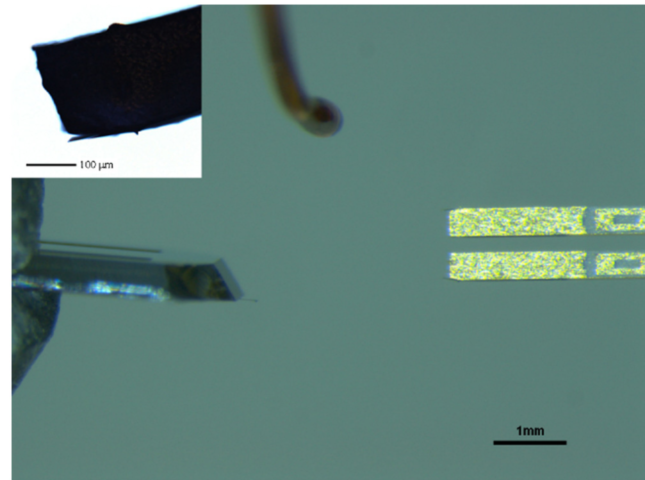

Fig. 4 Optical microscopy image of the cantilever chip, tuning fork, and gluing wire, as viewed under the stereo microscope. Inset: Optical microscopy image of a tuning fork tine with a tip attached.

tips is evaluated by electrical characterization and SPM imaging. We use commercial AFM chips (BudgetSensors®, TAP 300), which have a cantilever with a tip micromachined from silicon. Three micromanipulator stages are set up on a platform under a stereo microscope for tip mounting—one to hold the QTF, the second to hold the AFM chip, and the third to hold a thin copper wire with which to apply a small quantity of an ethyl cyanoacrylate—based adhesive (Super Glue®) near the end of the QTF tine. After the adhesive has been applied to the tine, the cantilever on the AFM chip is brought into contact with the adhesive and left for approximately 15 min to allow the adhesive to cure. The AFM chip is very carefully withdrawn, leaving the cantilever, with the tip, attached to the QTF tine. Figure 4 shows an optical microscope image of the AFM chip with the cantilever, the copper wire with the adhesive, and the QTF prior to attaching the cantilever and tip. The inset of Fig. 4 shows a higher magnification optical microscope image of the cantilever attached to the QTF tine.

The nominal resonance frequency of a QTF is dependent on its size, geometry, and the piezoelectric properties of

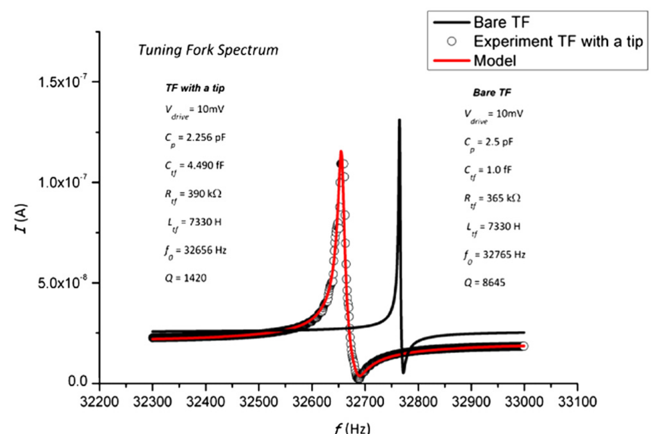

Fig. 5 Measured (circles) and modeled (red line) resonance curve of a QTF with an AFM tip attached to one of the tines. The resonance curve for a bare QTF is shown by the black line. Also listed are the QTF electrical parameters (see Table 2).

the quartz from which it was fabricated. The QTFs used here have a nominal resonance frequency of 32 768 Hz. It has been shown that an electronically driven QTF can be modeled by an equivalent RLC circuit.[17] A typical resonance curve of a bare QTF is shown in Fig. 5 (black line). The resonance frequency is slightly lower ($f_0 = 32\,765$ Hz)than the nominal one (32 768 Hz). In similar fashion, we have measured the resonance response of a QTF with a tip mounted at one of the tines and deduced the corresponding electronic parameters and the quality factor (Q) by fitting the equivalent RLC circuit model (red line) to the measured resonance curve (circles). The values of the QTF parameters are given in Table 2. Mounting the tip on a QTF reduces the resonance frequency of the QTF by approximately 100 Hz (less than 0.5%), while the Q is reduced by a factor of about five. The reason for the reduction in the resonance frequency is the extra mass due to the addition of a tip and glue, whereas the reduction of the Q is due to breaking of the QTF symmetry (tines are more mismatched). The asymmetry of the resonance curves in Fig. 5 is due to the presence of parasitic capacitance, C_p. It can be compensated using a variable capacitor or the QTF signal can be extracted from the RLC model. While the sensitivity of FM AFM is not affected by C_p, high Q values are desirable to achieve high sensitivity because the minimum detectable force gradient in FM AFM is proportional to $Q^{-1/2}$.[18]

3 System Integration

The components of the mSPM described above are integrated into a metrological frame, as shown in Fig. 1, which defines the coordinate system of the instrument. Experience in characterizing mSPMs at other metrology institutes[4–9] has shown that the metrological frame is the dominant source of measurement uncertainties arising from alignment errors, particularly Abbé errors and nonorthogonality of the measurement axes, and environmental vibration. To achieve the target total uncertainty of dimensional measurements, minimizing these contributions is a principal consideration in the design of the metrological frame and the material selected for its construction.

The following recognized principles have been used in the development of this design. The length of the metrology loop (that is, the mechanical distance between the tip of the probe and the point on the sample interacting with the tip) is minimized so that uncertainties arising from deformations or alignment errors in the structure are kept to a minimum. To achieve this objective, the integration into the metrology loop of translation stages for the coarse alignment of the sample in both the XY plane and along the Z-axis has been avoided. Furthermore, the two major components of the metrology loop, the metrological frame and the three axes translation stage, are precision engineered from SuperInvar, a FeNiCo alloy with a thermal expansion coefficient of $a = (-17 \pm 2) \times 10^{-8}$ K^{-1} at 20°C[19] and a temporal stability over a period of a day of $\Delta L/L = (0.00 \pm 0.03)$ part in 10^9 (Ref. 20). The metrological frame is axially symmetric around a vertical axis that runs through the tip to maintain the on-axis tip position even when the frame expands or contracts. Where possible, components are kinematically mounted, again to minimize distortions due to thermal expansion and to minimize displacement when the instrument is reassembled. Finally, the solid, rigid structure of the metrological frame minimizes the effects of ambient vibrations.

Accurate control of the environmental parameters such as temperature, atmosphere, and ambient vibrations is achieved by placing the mSPM structure in a chamber that allows operation in vacuum, controlled gas atmospheres, or air. The microscope and the beam delivery optics are mounted on a vibration isolation table that in turn rests on a pillar that is seismically decoupled from the laboratory building. The table is surrounded by a thermal enclosure that is flushed with thermalized, highly filtered air. The most significant heat source, the laser, is separated from the instrument by operating it in another room. Multiple temperature sensors and resistive heaters are embedded in the mSPM body to allow for the detection and active compensation of residual thermal gradients.

Table 2 The QTF electrical parameters deduced from fitting the measured resonance curves to a model of the equivalent RLC circuit. The abbreviations are as follows: C_p—parasitic capacitance, C_{tf}—QTF capacitance, R_{tf}—QTF resistance, L_{tf}—QTF inductance, f_0—QTF resonance frequency, Q—QTF quality factor. The resonance frequency and the Q are lowered by tip mounting. The QTF has been driven with a 10-mV peak-to-peak sinusoidal excitation. The values given here are representative for our QTF probes.

Equivavalent RLC circuit parameters	Bare tuning fork	Tuning fork with a tip
C_p	2.23 pF	2.5 pF
C_{tf}	4.5 fF	1.0 fF
R_{tf}	390 kΩ	365 kΩ
L_{tf}	7330 H	7330 H
f_0	32656 Hz	32765 Hz
Q	1420	8635

4 FM AFM Imaging

The first images with the mSPM have been acquired in FM AFM mode achieving truly non-contact tracking of the sample surface. A photograph of a QTF with a tip interacting

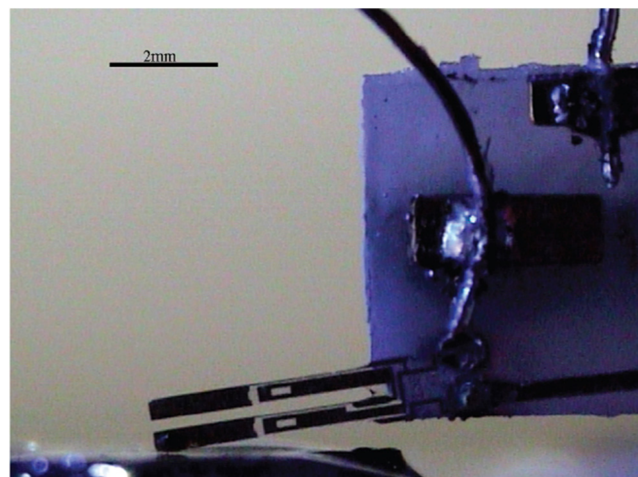

Fig. 6 Photograph of a QTF with a tip in contact with a sample.

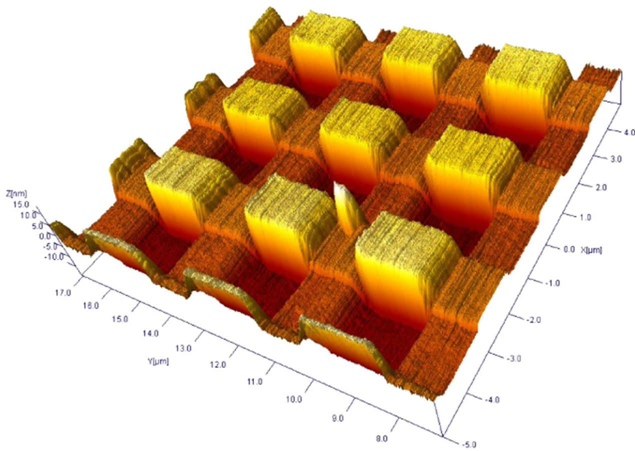

Fig. 7 SPM image of a two-dimensional grid artifact.

with a sample is shown in Fig. 6. In the FM AFM imaging mode, the QTF is electrically driven at the resonance frequency. As the tip approaches the surface, the tip-sample interaction shifts the resonance frequency of the QTF. The frequency error signal is measured by a phase locked loop that is then used in the feedback loop to control the *Z*-axis motion of the nanopositioning stage. The surface topography is reconstructed by mapping the three-dimensional motion of the nanopositioning stage as the surface is scanned.

The SPM imaging is done in a feedback loop, where typically the frequency error signal is below 1 Hz. Fine tuning of the control parameters is necessary to achieve optimal imaging in the FM AFM mode. A typical SPM image of a two-dimensional grid artifact taken with a relatively slow scan rate (0.2 Hz) under standard laboratory conditions is shown in Fig. 7. The following FM AFM parameters were used in acquiring the image—amplitude, $A = 89$ nm; drive frequency, $f_0 = 32\,565$ Hz; and frequency shift set point, $\Delta f = -17.3$ Hz. Currently, the influence of different FM AFM parameters on the imaging performance is being investigated. Drift characterization of the instrument with evaluation of the environmental effects (primarily temperature stability) is underway.

5 Conclusion

The design, construction, and preliminary evaluation of an mSPM are currently underway at NMIA. The mSPM will be the key instrument in a SPM metrology facility at NMIA, traceably linking dimensional measurements at the nanometer scale with NMIA's realization of the SI definition of the meter. This traceability will be achieved by measuring the displacement of the sample translation stage interferometrically in three dimensions using a frequency-stabilized laser that is referenced to NMIA's optical frequency comb.

The mSPM incorporates a QTF mounted tip for noncontact-mode AFM operation; a flexure-hinged, piezoelectrically actuated three-axis nanopositioning stage; and a plane mirror differential heterodyne interferometry system. To achieve a target combined uncertainty for the position measurement of less than 1 nm, the mSPM is designed to minimize uncertainties caused by thermal expansion and distortion, alignment errors, and environmental vibration. The instrument will be located on a vibration isolation table and will be enclosed in an acoustically shielding and temperature-controlled environmental chamber.

Preliminary evaluation of the nanopositioning stage indicates that with the planned load of intereferometry mirrors, sample stage, and sample, the stage is capable of providing sample motion suitable for AFM imaging. A reliable method to attach AFM tips to QTFs, developed at NMIA, allows the use of QTFs as noncontact FM AFM sensors when operating with an appropriate set of oscillation parameters. This has been confirmed by the acquisition of preliminary images of samples with the mSPM operating in FM AFM mode.

When completed and commissioned, the mSPM will be used primarily for calibrating transfer standard artifacts, which, in turn, will be used to calibrate a second SPM. This second instrument will be used for calibrating clients' transfer standard artifacts, for measuring and characterizing nanoparticles for NMIA's particle characterization laboratory, and for other research and development projects requiring measurement and imaging at the nanoscale.

References

1. Organisation Intergouvernementale de la Convention du Mètre, *The International System of Units (SI)*, 8th ed., 112, BIPM Sèvres (2006).
2. T. Udem, R. Holzwarth, and T. Hänsch, "Femtosecond optical frequency combs," *Eur. Phys. J. Spec. Top.* **172**(1), 69–79 (2009).
3. S. T. Smith and D. G. Chetwynd, *Foundations of Ultraprecision Mechanism Design*, Gordon and Breach, Amsterdam (1998).
4. G. Wilkening and L. Koenders, *Nanoscale Calibration Standards and Methods*, Wiley-VCH, Weinheim (2005).
5. H. U. Danzebrink et al., "Advances in scanning force microscopy for dimensional metrology," *CIRP Annals-Manufact. Technol.* **55**(2), 841–878 (2006).
6. K. R. Koops et al., "Calibration strategies for scanning probe metrology," *Meas. Sci. Technol.* **18**(2), 390–394 (2007).
7. V. Korpelainen and A. Lassila, "Calibration of a commercial AFM: traceability for a coordinate system," *Meas. Sci. Technol.* **18**(2), 395–403 (2007).
8. V. Korpelainen, J. Seppä, and A. Lassila, "Design and characterization of MIKES metrological atomic force microscope," *Precis. Eng.* **34**(4), 735–744 (2010).
9. J. A. Kramar, R. Dixson, and N. G. Orji, "Scanning probe microscope dimensional metrology at NIST," *Meas. Sci. Technol.* **22**(2), 024001–024011 (2011).
10. R. Koning, J. Flugge, and H. Bosse, "A method for *in situ* determination of Abbé errors and their correction," *Meas. Sci. Technol.* **18**(2), 476–481 (2007).
11. Model NPXYZ100A-I, npoint Inc., Madison, WI, USA.
12. F. J. Giessibl, "Advances in atomic force microscopy," *Rev. Mod. Phys.* **75**(3), 949–983 (2003).
13. F. J. Giessibl et al., "Subatomic features on the silicon (111)-(7 × 7) surface observed by atomic force microscopy," *Science* **289**(5478), 422–425 (2000), .
14. P. C. Gunther, U. Fischer, and K. Dransfeld, "Scanning near-field acoustic microscopy," *Appl. Phys. B* **48**(1), 89–92 (1989).
15. J. W. G. Tyrrell, D. V. Sokolov, and H. U. Danzebrink, "Development of a scanning probe microscope compact sensor head featuring a diamond probe mounted on a quartz tuning fork," *Meas. Sci. Technol.* **14**(12), 2139–2143 (2003).
16. A. Castellanos-Gomez, N. Agrait, and G. Rubion-Bollinger, "Dynamics of quartz tuning fork force sensors used in scanning probe microscopy," *Nanotechnology* **20**(21), 215502–215509 (2009).
17. Y. Qin and R. Reifenberger, "Calibrating a tuning fork for use as a scanning probe microscope force sensor," *Rev. Sci. Instrum.* **78**(6), 063704 (2007).
18. T. R. Albrecht et al., "Frequency modulation detection using high-*Q* cantilevers for enhanced microscope sensitivity," *J. Appl. Phys.* **69**(2), 668–673 (1991).
19. S. F. Jacobs, C. Johnston, and D. E. Schwab, "Dimensional instability of Invars," *Appl. Opt.* **23**(20), 3500–3502 (1984).
20. J. Berthold, III, S. F. Jacobs, and M. A. Norton, "Dimensional stability of silica Invar, and several ultralow-thermal expansion materials," *Metrologia* **13**(1), 9–16 (1977).

Bakir Babic joined the Nanometrology Section at the National Measurement Institute Australia (NMIA) as a research scientist in 2010. He received his PhD in nanoelectronics from the University of Basel, while working mainly on electronic transport characterization of single-wall carbon nanotubes under the supervision of Dr. C. Schonenberger and completed a postdoctoral fellowship at the Australian Institute for Bioengineering and Nanotechnology at the University of Queensland, working on a single biomolecule detector. He was also an SFN postdoctoral fellow at ETH Zurich, working with Dr. A. Imamoglu on quantum optics using carbon nanotubes.

Christopher H. Freund is an instrumentation engineer with the Nanometrology Section at the National Measurement Institute Australia (NMIA). His current role is the design and development of the metrological scanning probe microscope. He joined the group in 2007 after spending three years working in the area of optical standards, also at NMIA. He is a scientific instrument maker by trade and received his Mechanical Engineering Certificate in 1975. Until 2004, he was a member of the Optics Group of the Commonwealth Scientific and Industrial Research Organisation, where he began focusing on optical instrumentation design. His main interests are in computer-aided design, analysis software, and optical interferometry.

Jan Herrmann heads the Nanometrology Section at the National Measurement Institute Australia (NMIA). His team develops physical standards, instruments, and methods for measurement at the nanometer-length scale with a focus on the characterization of nanomaterials. He holds a doctorate in physics from the University of Leipzig. Before joining NMIA, he was a postdoctoral researcher at the University of California, San Diego, and a research scientist at Australia's Commonwealth Scientific and Industrial Research Organisation, with research interests that include superconductivity, electronic transport in nanostructures, and nano sensor applications.

Malcolm A. Lawn is a metrologist with the Nanometrology Section at the National Measurement Institute Australia (NMIA). Since joining the section in 2007, he has worked on establishing the scanning probe microscopy facility. He is a graduate in applied physics from the Royal Melbourne Institute of Technology. From 1991 to 2007, he was a member of the Time and Frequency Section at NMIA working on the development of a trapped ion frequency standard and data processing for precision time transfer via global positioning systems. His main interests are in atomic force microscope (AFM) calibration, calibration artifacts, and nanoparticle metrology with AFM.

John Miles received his PhD in solid state physics from Monash University in Melbourne in 1991. He is currently an honorary fellow at the National Measurement Institute of Australia (NMIA) and has more than 25 years experience in the fields of high-level dimensional, engineering, and mechanical measurements. He was actively involved in establishing NMIA's Nanometrology Program and recently served as Chairman of the Standards Australia Technical Committee NT-001 on Nanotechnology, having been Australia's Head of Delegation to ISO TC229 Nanotechnologies for many years.